The contribution of metal ions to the structural stability of the large ribosomal subunit

DANIEL J. KLEIN,[1] PETER B. MOORE,[1,2] and THOMAS A. STEITZ[1,2,3]

[1]Department of Molecular Biophysics and Biochemistry, [2]Department of Chemistry, Yale University, New Haven, Connecticut 06520-8114, USA

[3]Howard Hughes Medical Institute, New Haven, Connecticut 06520-8114, USA

ABSTRACT

Both monovalent cations and magnesium ions are well known to be essential for the folding and stability of large RNA molecules that form complex and compact structures. In the atomic structure of the large ribosomal subunit from *Haloarcula marismortui*, we have identified 116 magnesium ions and 88 monovalent cations bound principally to rRNA. Although the rRNA structures to which these metal ions bind are highly idiosyncratic, a few common principles have emerged from the identities of the specific functional groups that coordinate them. The nonbridging oxygen of a phosphate group is the most common inner shell ligand of Mg^{++}, and Mg^{++} ions having one or two such inner shell ligands are very common. Nonbridging phosphate oxygens and the heteroatoms of nucleotide bases are common outer shell ligands for Mg^{++} ions. Monovalent cations usually interact with nucleotide bases and protein groups, although some interactions with nonbridging phosphate oxygens are found. The most common monovalent cation binding site is the major groove side of G-U wobble pairs. Both divalent and monovalent cations stabilize the tertiary structure of 23S rRNA by mediating interactions between its structural domains. Bound metal ions are particularly abundant in the region surrounding the peptidyl transferase center, where stabilizing cationic tails of ribosomal proteins are notably absent. This may point to the importance of metal ions for the stabilization of specific RNA structures in the evolutionary period prior to the appearance of proteins, and hence many of these metal ion binding sites may be conserved across all phylogenetic kingdoms.

Keywords: RNA structure; ribosome structure; metal ion; coordination; magnesium; monovalent cation

INTRODUCTION

Metal ions such as magnesium (Mg^{2+}), sodium (Na^{+}), and potassium (K^{+}) serve important biological functions by interacting with nucleic acids, particularly RNA (for review, see Pyle 2002). Magnesium is especially suitable for neutralizing the negative charge density associated with the RNA phosphate backbone, for two reasons. First, it is the most abundant intracellular multivalent cation (Wacker 1969). Second, it has the highest charge density of all biologically available ions, owing to its relatively small ionic radius (0.6 Å). Two general modes of Mg^{2+} ion binding to RNA have been described: (1) a "diffuse binding" mode that involves nonspecific long-range electrostatic interactions with Mg^{2+} hexahydrate, and (2) a "site binding" mode that involves specific coordination of anionic ligands to partially dehydrated Mg^{2+} (Misra and Draper 1999). Both are important for the structural stabilization of RNA. Less is understood about the structural roles of monovalent cations, such as Na^{+} and K^{+}, in the stabilization of RNA structure. However, the cellular abundance of K^{+} and its specific structural requirement in at least two RNA molecules (Basu et al. 1998; Shiman and Draper 2000) suggest that it may also play an important role in the stabilization of the tertiary structure present in large RNA molecules.

It has been known for decades that the structure and function of the ribosome are strongly influenced by the presence of metal ions, especially Mg^{2+}. For example, the in vitro association of the small and large ribosomal subunits to form intact ribosomes depends strongly on Mg^{2+} ion concentration (Chao and Schachman 1956; Chao 1957; Tissieres et al. 1959). Further, growth of *Escherichia coli* cells under conditions of Mg^{2+} starvation result in ribosome depletion (McCarthy 1962), suggesting that Mg^{2+} is essential for the assembly and structural integrity of ribosomes.

Reprint requests to: Thomas A. Steitz, Department of Molecular Biophysics and Biochemistry, Yale University, 266 Whitney Ave., New Haven, CT 06520-8114, USA; e-mail: eatherton@csb.yale.edu; fax: (203) 432-3282.

Article and publication are at http://www.rnajournal.org/cgi/doi/10.1261/rna.7390804.

Consistent with this, replacement of Mg^{2+} with various polyamines in purified preparations of *E. coli* large ribosomal subunits results in irreversible unfolding and loss of peptidyl transferase activity (Kimes and Morris 1973). Other ribosomal functions influenced by Mg^{2+} include poly-U directed phenylalanine polymerization (Gordon and Lipmann 1967), polynucleotide binding to ribosomes (Moore 1966), and attachment of ribosomes to endoplasmic reticulum membranes (Khawaja and Raina 1970). However, it is difficult to assess the degree to which such effects are direct or indirect consequences of structural perturbations to the ribosome.

The importance of K^+ ions for ribosome structure and function is evident from the irreversible loss of poly-phenylalanine polymerizing activity and the significant unfolding that occurs when mammalian ribosomes are transferred to K^+-free buffers (Naslund and Huntlin 1970, 1971). Interestingly, *E. coli* ribosomes dissociate into subunits when exposed to high K^+ ion concentrations (Zitomer and Flaks 1972), most likely because K^+ ions compete with Mg^{2+} ions for metal binding sites at the subunit interface that strictly require Mg^{2+} for subunit association to occur.

Of all the ribosome and ribosomal subunit crystal structures reported to date, only the structure of the large ribosomal subunit from *Haloarcula marismortui* has been determined at a high enough resolution to permit the unambiguous identification of bound metal ions. In our previous work on the crystallographic refinement of the large subunit, we identified ~200 bound metal ions. With the exception of a single K^+ ion in the peptidyl transferase center (Nissen et al. 2000), none of the metal ions identified in the large ribosomal subunit had been described previously. Here we show that the metal ions in the large ribosomal subunit of *H. marismortui* bind to idiosyncratic folds in RNA, thereby mediating interactions both within and between the individual domains of 23S RNA. Metal ions are particularly concentrated in the conserved functional regions of 23S RNA, and they tend to stabilize RNA structure in regions where ribosomal proteins are notably absent.

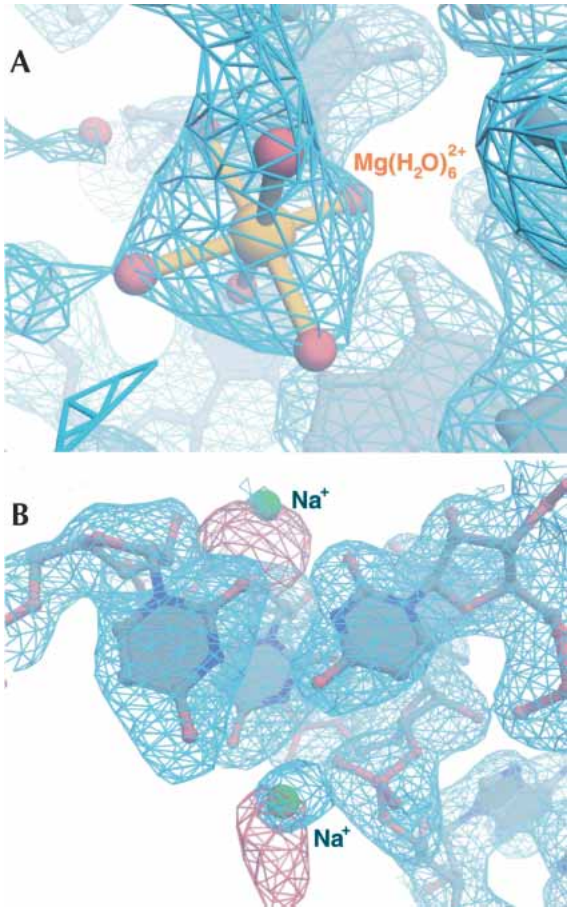

FIGURE 1. (*A*) Experimental electron density map contoured at 0.8σ (blue mesh) showing typical electron density for a Mg^{2+} ion (gold). Water molecules of the inner-sphere octahedron are displayed as red spheres connected to a central Mg^2+ ion with gold bonds. (*B*) Region of the experimental map (blue mesh) contoured at 0.8σ showing typical density for two Na^+ ions (green). The corresponding region of an experimentally phased isomorphous difference map contoured at 4σ (red mesh) and calculated with coefficients corresponding to $|F_{obs(Rb+)}| - |F_{obs(native)}|$ to a resolution of 3.7 Å is superimposed.

RESULTS

Identification of metal ions in the large ribosomal subunit

The exceptional quality of both the experimentally phased electron density map and that obtained with calculated phases and $2F_{obs} - F_{calc}$ amplitudes allowed unambiguous identification of 116 Mg^{2+} ions based on electron density features (Fig. 1A). Initially, a list of candidate electron density peaks for partially dehydrated Mg^{2+} ions was generated automatically by searching $F_{obs} - F_{calc}$ difference electron density maps for peaks that were 1.9–2.1 Å from RNA or protein N or O atoms. Each peak so identified was inspected to determine whether the arrangement of surrounding electron density features in experimentally-phased and $2|F_{obs}| - |F_{calc}|$ maps was octahedral. Mg^{2+} ions were modeled into all such peaks. The modeling of water molecules coordinated to the inner sphere of Mg^{2+} ions was also based on electron density features in $F_{obs} - F_{calc}$ difference maps, and the typical refined distances of ~2.0 Å between the ions and such water molecules validated our identification of Mg^{2+}. Fully hydrated Mg^{2+} ions, which would not be identified by the automated search, were found by searching electron density maps visually for peaks containing six identifiable water molecules arranged octahedrally (Fig. 1A). Replacement of $MgCl_2$ by $MnCl_2$ in the crystallization buffers would have been useful for identification of bound Mg^{2+} ions, but this experiment was not possible for the *H. marismortui* large ribosomal subunit, because replacement of $MgCl_2$ by $MnCl_2$ invariably caused the crystals to become twinned.

Bound monovalent cations were identified and modeled at sites of significant isomorphous difference electron density between crystals of the *H. marismortui* large ribosomal subunit soaked in stabilization buffers containing rubidium chloride (RbCl) and native crystals prepared in buffers in which the only monovalent cations were Na^+, K^+, and NH_4^+ (Fig. 1B). Of the 88 monovalent cations located this way, 86 were modeled as Na^+ and only two as K^+. There are two reasons for this. First, it is very difficult to differentiate between Na^+, K^+, and NH_4^+ in native electron density maps at the current resolution (2.4 Å). However, most of the monovalent cation binding sites found are likely to be occupied with Na^+, because the crystals of the *H. marismortui* large subunit used for high-resolution data collection were stabilized in buffers containing a large excess of Na^+ over K^+ and NH_4^+. Second, when K^+ was modeled into most monovalent binding sites, unusually high temperature factors for the ion emerged after refinement, whereas when Na^+ was modeled into these sites, ion temperature factors were consistent with those of the other atoms in the surrounding area. The two monovalent binding sites in which K^+ was modeled behaved differently. The corresponding electron density peaks were larger, and upon refinement, temperature factors more consistent with those of surrounding atoms emerged. It is likely that most of the monovalent binding sites we identified in the large ribosomal subunit are occupied with K^+ under physiological conditions, where K^+ predominates over Na^+.

The binding sites for magnesium ions in the large ribosomal subunit

The 116 Mg^{2+} ions in the structure of the *H. marismortui* large ribosomal subunit can be classified into groups based on the geometric arrangement of RNA and protein atoms inner-sphere coordinated to them (Table 1). Magnesium ions are observed to have zero (type 0), one (type I), two (type II), three (type III), four (type IV), and five (type V) inner-sphere RNA or protein ligands (Fig. 2), but never six. Mg^{2+} ions of type II and type III can be divided into two subgroups based on the three-dimensional arrangement of their RNA or protein ligands. In Mg^{2+} ions of type IIa, the inner-sphere contacts to RNA or protein are orthogonal (Fig. 2C), whereas in Mg^{2+} ions of type IIb the inner-sphere contacts to RNA or protein are located on opposite corners of the coordination octahedron (Fig. 2D). In Mg^{2+} ions of type IIIa, the RNA or protein atoms of the inner-sphere coordination octahedron all lie in a single plane that includes the Mg^{2+} ion (Fig. 2E), whereas in Mg^{2+} ions of type IIIb the three inner-sphere contacts to RNA or protein are mutually orthogonal (Fig. 2F). Only single examples of Mg^{2+} ions of types IV and V were identified in the large ribosomal subunit. Finally, there proved to be five Mg^{2+} ions that appear to have nonoctahedral coordination geometries, and that are consequently grouped into a final class, type X. Type X Mg^{2+} ions are usually in places where it is difficult to locate coordinated waters, and local disorder may blur the electron density.

The frequencies with which each type of Mg^{2+} ion are observed in the large ribosomal subunit are reflective of the roles played by Mg^{2+} in the stabilization of the structure of 23S RNA. Mg^{2+} ions of type IIa are the most common, with 40 examples (34.5%), followed by Mg^{2+} ions of type I with 37 examples (31.9%). Mg^{2+} ions of both classes are often bound to RNA secondary structure motifs wherein the phosphate groups of two consecutive nucleotides require charge neutralization due to their close juxtaposition. Magnesium ions of type 0 are rare in the large subunit (nine occurrences), but like type IIa and type I ions, type 0 ions usually bind to specific parts of RNA secondary structure motifs, such as the major groove of an A-form RNA helix. Mg^{2+} ions of type IIb (five examples) are much less common than those of type IIa, and never make inner-sphere contacts with consecutive residues. Instead, they usually stabilize anionic groups from nonconsecutive nucleotides in idiosyncratic RNA secondary structure motifs, and in a few cases stabilize tertiary interactions between nucleotides that are far separated in sequence. Finally, Mg^{2+} ions of types IIIa, IIIb, IV, and V together represent 17.2% of the total. Many of the 20 Mg^{2+} ions in these classes are bound to highly idiosyncratic binding sites in 23S RNA that are unlike any previously reported.

We did not consider outer-sphere contacts with RNA or protein in the classification of Mg^{2+} ions, because such considerations introduce tremendous complexity to the nature of the Mg^{2+} binding sites observed in the large ribosomal subunit, thereby precluding simple classification. Nonetheless, outer-sphere contacts are surely important in determining the binding specificity of Mg^{2+} ions as well as for the neutralization of buried negative charges. This is apparent from the simple observation that the number of outer-sphere contacts in the large subunit is much larger than the number of inner-sphere contacts (378 vs. 200). When the identities of the RNA and protein ligands that make the outer-sphere contacts with Mg^{2+} are compared to those that make inner-sphere contacts, a few general principles became apparent. Nonbridging phosphate oxygen atoms of the RNA phosphodiester backbone account for most of the inner-sphere ligands of Mg^{2+} ions (73%) but only ~50% of the outer-sphere ligands. Conversely, the functional groups of nucleotide bases, particularly the 7-imino groups of A and G, are outer-sphere ligands for Mg^{2+} much more often than they are inner-sphere ligands (63 vs. 11 for the 7-imino group). Further, contacts between Mg^{2+} ions and ribosomal proteins are more often made through the outer sphere (32 contacts) than through the inner sphere (13 contacts) of Mg^{2+} ions.

In addition to the important contribution of the positioning of RNA and protein functional groups in creating binding sites for Mg^{2+} ions, as emphasized in our classifi-

TABLE 1. Summary of magnesium ion contacts in the *H. marismortui* large ribosomal subunit

Mg^{2+}	Inner sphere contacts	Outer sphere contacts	Class
38		2115 O4, 2116 O4, 2271 N7, 2274 N7, 2275 N7, 2275 O6, 2276 O4	0
55		2720 OP1, 2721 OP2, 2721 OP1, 333 OE2 (L3), 333 OE1 (L3), 32 CO (L24e)	0
63		1363 O6, 1363 N7, 1364 O6	0
65		782 O2′, 783 OP1, 15 CO (L2), 17 CO (L2), 179 CO (L2), 180 CO (L2), 182 CO (L2), 184 CO (L2)	0
71		1813 O4, 1815 OP1, 1816 OP2, 1817 O4, 1818 N3, 1818 N4	0
76		1418 O2′, 1419 OP2, 1443 N7, 1443 O6, 1444 O6, 15 OD1 (L32e)	0
100		2064 O4, 2079 N7	0
107		1977 OP1, 1978 OP1, 1986 O6, 2000 N7	0
114		1848 OP2, 1849 OP2	0
12	28 OP1	1304 OP1, 1305 OP1, 1305 OP2, 1343 OP2, 1344 OP1	I
17	456 OP2	455 OP2, 455 OP1, 457 OP1, 458 OP1, 85 CO (L4), 86 CO (L4)	I
19	2011 OP2	1890 O2′, 1891 OP2, 1891 O6, 1891 N7, 1892 N4, 1941 OP2	I
20	1830 OP1	1828 N3, 1828 O2′, 1828 N2, 1831 OP1, 1832 O6, 1842 OP1, 1842 OP2	I
21	2304 OP2	2301 OP2, 2303 OP1, 2304 N7, 2305 N7, 2305 OP2, 2306 O4	I
24	1381 N7	1380 O2′, 1380 OP1, V23 ND1	I
32	2115 OP1	2116 OP2, 2272 OP1, 2273 OP2, 196 CO (L2), 199 CO (L2)	I
35	1484 OP2	1455 OP2, 1456 OP2, 1457 O4, 1484 N7, 1485 OP2	I
36	956 OP1	955 OP1, 955 OP2, 956 N7, 957 N7, 1006 OP1, 1006 OP2	I
37	2553 OP2	2552 O2′, 2554 OP2, 2575 OP1, 2576 OP2, 2576 N7	I
39	115 OP1	112 OP2, 114 O2′, 117 N7, 118 N7, 118 O6, 119 N6	I
40	392 OP2	171 OP1, 172 OP1, 391 OP2	I
45	1979 OP1	1998 OP1, 1999 OP1, 1999 OP2	I
46	1794 N7	1793 OP2, 1794 OP1, 1796 OP1, 1796 OP2	I
47	1098 OP2	1097 OP1, 1099 O6, 1099 N7, 125 CO (L30)	I
50	2248 OP2	2247 OP1	I
51	641 OP2	641 N7, 642 N7, 1355 N3, 1355 OP2	I
53	471 O6	469 O2′, 470 O4, 881 O2′, 882 OP2, 883 O4, 888 O2′	I
58	2013 OP1	1883 OP2, 1884 OP1, 2626 OP1, 207 OE1 (L2) 207 CO (L2)	I
59	2618 OP1	2619 OP2, 2641 OP2, 2642 OP2, 2642 N7, 2643 O6, 2643 N7	I
60	175 OP2	172 OP1, 173 OP2, 173 OP1, 225 OP1, 392 OP1, 393 OP1, 393 OP2	I
68	2568 OP2	2567 OP1, 2567 OP2, 2568 N7, 2569 N7, 2569 OP2, 2569 N6	I
69	42 OD1 (L14)	1749 OP2, 2546 OP1, 2583 OP1, 2584 OP2	I
72	954 OP1	2298 OP1, 2299 OP2, 2301 OP1	I
83	1754 OP2	1753 OP2, 1754 N7, 1755 N7, 1755 OP2	I
84	1742 OP2	1742 N7, 1743 O6, 1743 N7, 1744 N7, 1744 O6, 1745 O6, 2033 OP1, 2033 N7	I
85	2618 OP1	2617 O2′, 2641 OP2, 2641 OP1, 2642 OP2	I
90	2103 OP2	2102 OP2, 2479 N7	I
91	918 OP1	2293 OP1, 2391 OP1, 2465 N7, 2465 OP2	I
92	1844 OP2	1843 OP1, 1845 N6, 1845 N7, 1845 OP2	I
98	907 N7	906 OP2, 907 OP2, 907 N6	I
105	817 O6	795 O6, 816 N7, 816 OP2, 817 N7, 90 OG (L19e)	I
110	2609 N7	2606 O6, 2606 N7, 2609 O6, 2609 OP2, 2610 O4	I
111	187 N1	155 OP1, 188 O2, 206 O2′, 207 OP1, 438 O2	I
112	2112 N7	2112 OP2, 2112 N6, 2113 O6	I
113	2430 N1	220 OP1, 2430 N6, 2431 N3, 2431 O2, 2468 OP1	I
115	1850 O4	1849 N7	I
4	456 O6, 459 OP1	455 N7, 455 OP2, 456 N7, 460 OP1, 477 OP1	IIa
9	2611 OP1, 2612 OP1	2093 OP2, 2094 OP1, 2094 OP2	IIa
11	824 N7, 854 N7	823 OP2, 824 O6, 824 OP2, 853 OP2, 854 O6, 854 OP2	IIa
13	877 OP1, 2623 OP1	885 O6, 2475 OP2, 2624 OP2, 195 OD1 (L2)	IIa
14	2102 OP2, 2537 OP2	2101 O2′, 2101 N3, 2480 N7, 2536 O2′	IIa
18	1291 OP2, 1292 OP2	909 OP2, 910 OP2, 911 O6, 1292 N7	IIa
22	2097 OP2, 2540 OP2	2095 OP2, 2096 O2′, 2097 N7	IIa
23	2617 OP2, 2618 OP2	2616 O2′, 2618 N7	IIa
25	1120 OP2, 1121 OP2	1121 N7, 1238 OP1	IIa
27	240 OP1, 269 O6	267 OP2, 268 OP1, 269 N7, 146 NE2 (L15e)	IIa
28	1448 OP2, 1677 O4	1676 N7, 1676 O6, 54 CO (L23)	IIa
29	1503 OP2, 1679 OP2	1504 OP2	IIa

TABLE 1. *Continued*

Mg^{2+}	Inner sphere contacts	Outer sphere contacts	Class
30	1748 OP2, 1749 OP1	2584 OP2, 2585 OP2	IIa
31	777 OP2, 778 OP2		IIa
34	2302 OP1, 2303 OP1	2301 N3, 2304 O6, 2305 N6	IIa
42	1309 O2, 1346 O2	1309 O2′, 1346 O2′	IIa
43	816 O6, 817 O6	795 O2′, 815 OP2	IIa
48	2746 OP2, 2750 OP2	2745 OP1, 2745 OP2, 2749 OP2	IIa
49	2421 OP1, 2423 OP1	2402 OP1	IIa
54	162 OP1, 2276 OP1	163 OP2, 169 OP2	IIa
56	2757 OP1, 335 CO (L3)	2719 OP2, 2720 OP2, 2758 OP2, 337 CO (L3)	IIa
61	1369 OP2, 2650 OP2	1371 O2′, 2649 OP1	IIa
66	1873 OP2, 26 OD2 (L2)		IIa
70	166 OP2, 219 O6	165 O2′, 219 N7, 221 N3	IIa
74	1286 OP1, 1287 OP1	1287 N7, 71 OE1 (L30), 72 CO (L30), 73 CO (L30), 75 CO (L30)	IIa
75	907 O2′, 908 O4′	907 N3, 1270 OP2, 1328 N6	IIa
80	1684 OP1, 1724 OP1	1431 OP1, 1691 N3, 1722 O2	IIa
86	532 OP1, 533 OP2	10 O4, 534 OP1, 2814 N1	IIa
87	682 OP2, 683 OP2	683 N7	IIa
88	2540 O6, 2611 O2′	2540 N7, 2612 OP2, 2614 OP1, 2646 OP2, 2647 N4	IIa
93	1070 O2′, 1071 OP1	627 OP1, 913 N6, 914 N1, 1071 N7	IIa
95	956 OP2, 957 OP2	921 O6	IIa
96	1848 O6, 1849 O6	1847 OP2, 1848 N7, 1849 N7, 1883 O4	IIa
97	863 O6, 864 O4	782 O6, 862 O4, 863 N7	IIa
101	2281 OP2, 2282 O4	2107 OP1, 2286 OP1	IIa
102	2434 N3, 2458 O2	2434 O2′, 2458 O2′, 66 OD1 (L44e)	IIa
103	2578 OP2, 2579 OP1		IIa
104	2104 OP1, 2105 OP2	2474 OP1, 2474 OP2	IIa
106	1106 OP1, 1107 OP2	1103 OP1, 1104 OP2, 1107 N7	IIa
109	903 OP1, 1357 N7	622 O2′, 904 OP1, 1356 O2′, 1357 N6	IIa
15	844 OP1, 1689 OP1	844 N7, 882 N1, 1688 O2′, 1689 N7, 1690 N4, 1692 N3, 5 OG (L37e)	IIb
52	1125 OP2, 92 OP1 (5S)	1126 OP2, 1129 O2, 1129 N3, 90 O6 (5S), 92 OP2 (5S)	IIb
62	1489 OP2, 1491 O6	1487 OP2, 1488 OP1, 1490 OP2, 1490 N7, 1491 N7	IIb
77	880 OP1, 883 OP2	882 OP1, 884 OP2, 1836 N6, 1836 N7	IIb
94	1096 OP2, 1257 OP2	1258 N7	IIb
1	2483 OP2, 2533 OP2, 2534 OP2	2482 O2′, 2484 OP2, 2532 O2′	IIIa
3	876 OP2, 877 OP2, 2624 OP1	193 CO (L2), 195 OD1 (L2)	IIIa
6	821 OP1, 822 OP2, 854 OP1	855 OP2, 856 OP1	IIIa
16	1504 OP1, 1678 OP1, 1679 OP1		IIIa
26	2608 OP1, 2609 OP1, 2610 OP2	2542 OP1	IIIa
64	2277 O4, 2278 O4, 2471 O6	2113 O6	IIIa
78	45 CO (L44e), 47 CO (L44e), 49 OD1 (L44e)	2121 OP1, 2122 OP1	IIIa
79	165 N7, 167 OP1, 168 OP2	164 N7, 164 OP2, 165 OP2	IIIa
89	516 OP2, 517 OP2, 518 N7		IIIa
108	133 CO (L32e), 136 CO (L32e), 139 CO (L32e)	137 CO (L32e)	IIIa
116	1840 O2′, 1841 OP2, 2022 N7	1840 N3, 2022 OP2	IIIa
2	627 O6, 2483 OP1, 2534 OP1	625 O2′, 626 O4	IIIb
5	1836 OP1, 1838 OP1, 1839 OP1	1837 OP1	IIIb
7	832 OP2, 1839 OP2, 1840 OP2	833 OP1	IIIb
8	919 OP1, 2464 OP1, 2465 OP1	2466 OP2	IIIb
10	836 OP1, 2615 OP1, 230 OE1 (L3)	2616 OP2, 230 CO (L3)	IIIb
41	196 OP1, 227 O2′, 228 O4′	227 N3	IIIb
81	1420 OP1, 1421 OP2, 1438 OP2		IIIb
33	1747 OP1, 1748 OP1, 1749 O4, 2585 OP1 37 OE1 (L24), 111 CO (L24), 112 CO (L24)	2586 OP2	IV
73	114 CO (L24), 117 CO (L24)	35 CO (L24)	V
44	2048 OP1, 2089 OP1, 65 CO (L22)	2047 OP1	X
57	1883 OP2, 2012 O2′, 207 CO (L2)		X
67	1845 OP1, 1846 OP1, 1884 O6, 188 CO (L2)	1883 O4	X
82	1437 OP2	1424 N7, 1424 OP2, 1425 N7, 1436 OP2	X
99	2612 O2′	2647 OP2, 2648 OP2	X

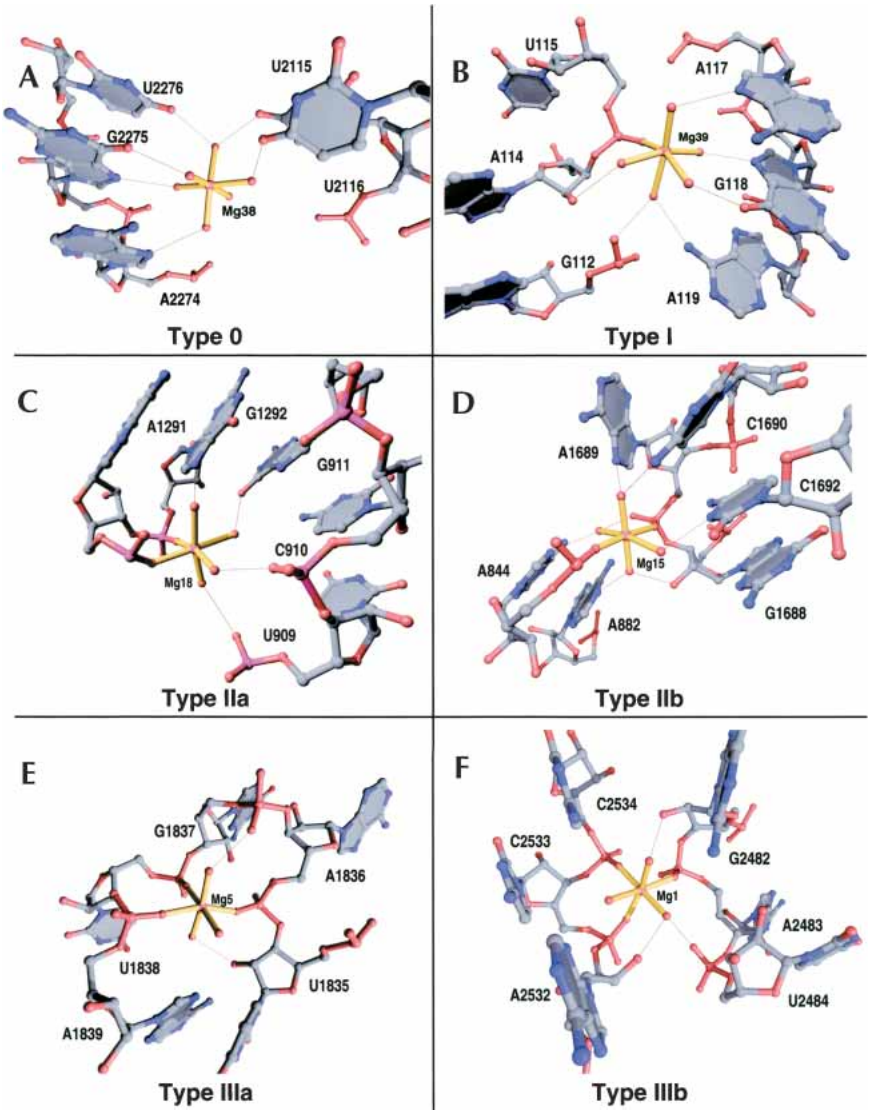

FIGURE 2. Examples of each of six distinct geometric classes of Mg^{2+} ions observed in the large ribosomal subunit. The inner-sphere coordinations of each Mg^{2+} ion are represented with gold bonds. The outer-sphere coordinations of each Mg^{2+} ion are represented with thin black lines.

cation scheme, it is important to point out that other factors, including metal ion hydration and the electrostatic potential of local macromolecular environments, are also critical factors that determine the binding sites for metal ions.

The binding sites for monovalent cations in the large ribosomal subunit

Monovalent cations, such as Na^+ and K^+, lack a preferred coordination geometry. Therefore, their coordination geometries preclude a classification scheme analogous to that proposed for Mg^{2+}. The 88 monovalent cations in the structure of the *H. marismortui* large subunit can, however, be classified according to their binding sites. When so classified, four different categories emerge: (1) those that bind in the major groove of RNA helices, (2) those that bind exclusively to ribosomal proteins, (3) those that bind at interfaces between ribosomal proteins and RNA, and (4) those that bind to idiosyncratic RNA structural motifs (Table 2).

The most common type of monovalent cation binding site in 23S RNA is that provided by the electronegative major groove edge of guanosines, often in the structural context of G-U wobble base-pairs, with a G-C base pair stacked on one or both of its sides (Fig. 3A). The monovalent cation usually lies in the same plane as the G-U wobble base pair and contacts the O6 of G and O4 of U, while also contacting the O6 of another G immediately adjacent to the U of the wobble pair (Fig. 3A).

Two structural features appear to engender specificity for monovalent cations in 23S RNA metal ion binding sites: (1) arrangement of electronegative functional groups are inconsistent with the octahedral geometry Mg^{2+} ions require (Fig. 3B), and (2) the coordination distances between the ion and its RNA ligands are appropriate only for a monovalent cation (Fig. 3B). We typically find the coordination distances between Na^+ ions and RNA ligands to be between 2.8 Å and 3.2 Å, which is significantly larger than the inner-sphere coordination distance required by Mg^{2+}, but not large enough to accommodate a fully hydrated Mg^{2+} ion.

An examination of the identities of the RNA and protein ligands that coordinate the monovalent cations in the large ribosomal subunit reveals further differences between the binding sites for monovalent and divalent cations. Unlike the inner-sphere contacts to Mg^{2+} ions, we find that inner-sphere contacts to Na^+ and K^+ commonly involve electronegative functional groups on nucleotide bases and ribosomal proteins. For example, Na^+ and K^+ ions make many more contacts with functional groups on nucleotide bases (138) than they do with the nonbridging phosphate oxygen atoms of the RNA backbone (55). In this respect, Na^+ and K^+ and the coordinated water molecules of partially hydrated Mg^{2+} ions behave similarly. This finding is consistent with the results of Doudna and colleagues, who demonstrated that monovalent cations can

TABLE 2. Summary of monovalent cation contacts in the *H. marismortui* large ribosomal subunit

Na+/K+	Sites of RNA & protein contact
1	1069 OP2, 1072 N7, 1097 O6
2	1119 O2′, 1120 OP2, 1121 O6, 1122 O4
3	643 OP2, 644 OP2, 904 O4, 1354 OP1
4	45 OD1 (L4), 94 CO (L4), 96 CO (L4)
5	630 N3, 630 O2′, 631 O2′
6	2093 N7, 2094 N7, 2649 N1
7	40 O2, 40 O2′, 41 O4′, 442 N1, 443 O2
8	1394 O2, 1432 O4, 1724 O2
9	1133 O2′, 1134 O1P, 154 CO (L10e), 157 CO (L10e), 159 CO (L10e)
10	2577 N3, 2577 O4′, 2578 N7, 2579 N7, 2579 O6
11	2524 N7, 2525 N7
12	61 OE2 (L24), 7 NE2 (L24)
13	2399 O6
14	2607 O2, 2607 O2′
15	165 OP2, 166 O2′, 167 OP1
16	896 O2, 896 O2′, 897 O4′
17	1416 O3′, 1416 O2′, 1417 OP1, 42 CO (39e), 45 CO (39e)
18	2543 N7, 2544 N7
19	2466 OP1, 2466 N7, 36 CO (L15)
20	2543 O6, 2615 O4
21	837 OP1, 1736 OP1, 229 CO (L3)
22	114 NH1 (L10e)
23	885 O2′, 2112 N3, 2475 N4
24	45 O2′, 130 O2, 146 O4, 147 O6
25	776 O2′, 777 OP2, 779 O4
26	1971 O6, 2009 OP2, 2010 OP2, 2012 O4
27	821 OP1, 854 OP1, 1831 O2′, 1831 O3′
28	56 O6, 59 N3, 61 N7, 61 O6
29	66 OP2, 107 O4, 108 O2
30	141 O2, 141 O4′, 142 O6, 142 N7
31	170 O2, 171 O4′, 218 O2′, 221 O6
32	386 O6, 387 O6, 388 O6, 402 O4
33	1894 O2, 1897 O4, 1898 O6, 1939 O4
34	1894 O4′, 1894 O2, 1896 O6, 1896 N7
35	622 O6, 623 O4, 628 O2′, 630 OP2
36	1706 O6, 1707 O6
37	70 CO (L22), 72 CO (L22)
38	2659 O3′, 2660 OP1, 72 CO (L22), 75 CO (L22)
39	2540 O6, 2616 O6, 2645 O2, 2645 O2′
40	1740 O4, 1741 O4, 2033 O2′
41	681 O2′, 682 OP2, 683 N7, 683 O6
42	892 N7, 893 O2, 893 O2′
43	308 O4, 335 O2′, 335 O2, 342 O2, 94 OG (L24), 95 OD1 (L24)
44	2811 O2′, 2812 OP2, 2816 O2′, 2817 OP2, 2663 O2
45	201 CO (L2), 203 CO (L2), 208 CO (L2)
46	60 CO (L13), 61 CO (L13), 63 CO (L13), 69 CO (L13)
47	106 CO (L15e), 106 OG (L15e), 109 CO (L15e), 112 CO (L15e)
48	20 CO (L21e), 22 CO (L21e), 24 OG (L21e), 46 OG (L21e)
49	914 O3′, 914 O2′, 915 OP2, 1043 O3′, 1045 OP1
50	623 O2′, 623 O2, 624 O4′, 901 OP1
51	40 N3 (5S), 40 O2 (5S)
52	955 O2′, 80 OP1 (5S)
53	1040 O2′, 1296 OP1, 14 CO (L15)
54	769 O4′, 768 O2′, 2112 OP1
55	1119 O6, 1243 OP1, 47 CO (L13)
56	920 O2, 920 N3, 2278 OP1, 2279 O4′
57	941 O6, 942 O4, 1024 O6
58	2611 OP1
59	922 OP2, 923 O2′, 924 O4′, 2109 OP2
60	453 O2′, 453 O3′, 454 OP2, 478 OP1, 479 OP2
61	837 OP1, 230 CO (L3)
62	168 OP1, 2110 OP2, 2111 OP1, 2277 OP1
63	1359 O2′, 1360 OP1
64	2057 O4, 2058 O6
65	391 O2, 398 O2, 391 O2′, 392 O4′, 399 O2, 193 CO (L15e)
66	544 O6, 545 O6, 611 O6
67	464 O6, 475 OP2, 55 CO (L4)
68	798 O6, 815 O4, 814 O6
69	391 O4, 398 O4, 395 OP2, 392 O2
70	1832 OP2, 2022 OP2
71	2491 O6, 2492 O4, 2529 O6
72	919 O4, 924 O6
73	1576 O6, 1577 O4, 1618 O6, 1619 O6
74	196 O6, 196 N7, 415 O2′, 416 O4′
75	868 O2′, 887 OP2, 886 O2′, 869 OP2, 869 N7
76	633 OP1, 2538 OP1, 2539 OP1
77	1295 O6, 1293 OP2
78	903 O4, 902 O6, 18 CO (L15)
79	831 O2, 832 O4, 833 O6, 27 CO (L15), 28 CO (L15), 29 CO (L15), 31 CO (L15), 33 CO (L15), 39 OE1
80	(L15)
81	2585 O6, 2586 O4, 2587 O4, 2592 O6
82	2772 O6, 2773 O6
83	21 O6 (5S), 22 O6 (5S), 55 O2 (5S), 57 N1 (5S), 58 N7 (5S), 58 O6 (5S)
84	197 N3
85	1077 N7, 1077 O6, 1079 OP1
86	12 O2′, 60 CO (L22), 63 CO (L22)
K1	2102 O6, 2102 N7, 2482 O6, 2482 N7
K2	162 OP2, 163 O4, 172 O4

replace hydrated Mg^{2+} in a fragment of the signal recognition particle RNA, and that when this occurs the monovalent cation binds to a site formerly occupied by one of the water molecules coordinated to Mg^{2+} (Batey and Doudna 2002).

Small structural motifs in RNA that bind metal ions

The structural motifs in 23S RNA that form the binding sites for metal ions are largely idiosyncratic, due to the complex tertiary folding of 23S RNA. The common feature of many sites in 23S RNA that bind metal ions is the presence of helical bulges and interhelical junctions that break the continuity of A-form helical stacking. These regions result in short stretches of grossly distorted RNA backbone structure that inevitably position electronegative anionic ligands in close proximity. The metal ions found at such sites stabilize the RNA structure by neutralization of negative charge density.

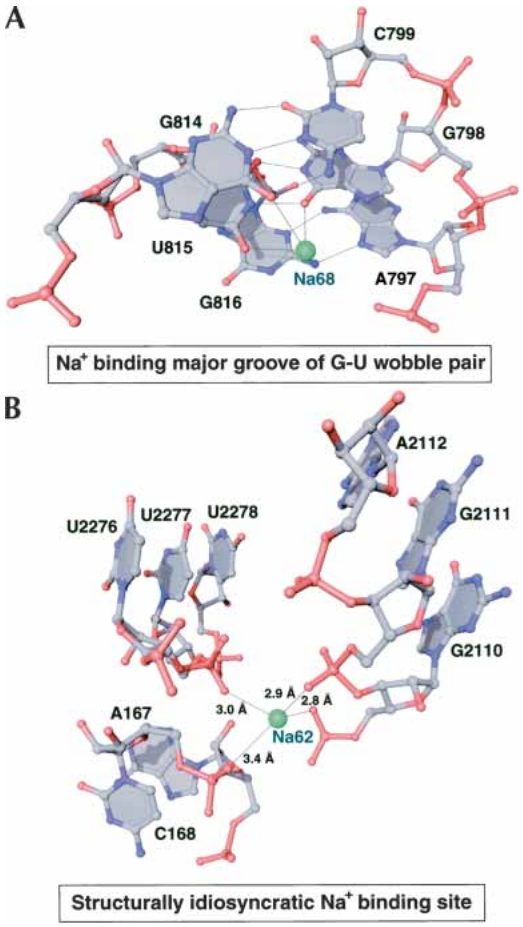

FIGURE 3. Common binding sites for monovalent cations in the large ribosomal subunit. RNA is shown in a ball-and-stick representation with Na^+ ions as green spheres. Thin black lines are shown between functional groups in the RNA that are observed to coordinate the Na^+ ions.

Despite the structural idiosyncrasy of most binding sites for metal ions in the large ribosomal subunit, a number of metal ions bind small motifs in 23S RNA secondary structure that may in fact be considered general metal ion-binding motifs. We identified two examples of putative small RNA motifs that bind either a monovalent cation or a Mg^{2+} ion.

There is a single example of an AA-platform motif present in the structure of 23S RNA. We identified a Na^+ ion located immediately beneath this platform that appears to make a number of stabilizing interactions (Fig. 4A). This Na^+ ion is coordinated to the 3-imino and 2′-hydroxyl groups of the 5′-A of the AA-platform, the 6-oxo and 7-imino groups of a G immediately 3′ to the AA-platform, and the 6-oxo group of an additional G that is stacked beneath the 5′-A of the AA-platform. Interestingly, our observation of a monovalent cation stabilizing an AA-platform motif parallels the identification of a critical K^+ ion bound to a similar AA-platform present in the group I intron RNA (Basu et al. 1998). The K^+ ion in the group I intron RNA is coordinated to the 2′-hydroxyl of the 5′A of the AA-platform, the pro(R) nonbridging phosphate oxygen of the 3′A of the AA-platform, the 6-oxo and 7-imino groups of a G immediately 3′ to the AA-platform, and the 4-oxo group of an additional U (Fig. 4B). Although subtle differences in the precise coordination of the monovalent cations in each of these AA-platforms exist, these structures support the hypothesis that a monovalent cation is important for the stabilization of AA-platforms.

One small Mg^{2+}-binding motif in 23S RNA that binds Mg^{2+} ions consists of a noncanonically base-paired G that contacts the phosphate group of an adjacent RNA strand. The structural consequence of this arrangement of nucleotide bases is the formation of a type IIa binding site for a Mg^{2+} ion that coordinates the 6-oxo group of G and the pro(S) phosphate oxygen of the nucleotide 5′ to the site of interaction between the 2-amino of the G and the phosphate group (Fig. 5). The two examples of this type of Mg^{2+} binding motif observed in the structure of the large ribo-

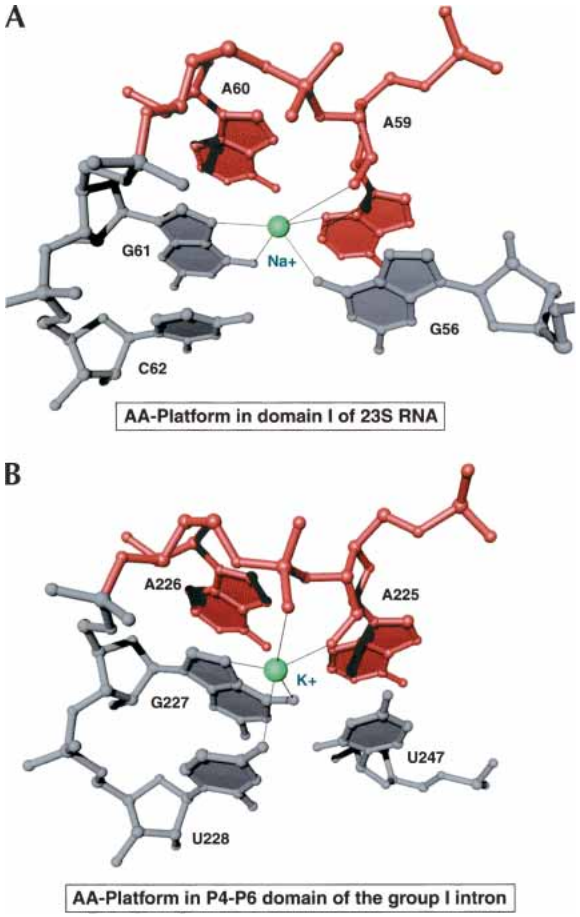

FIGURE 4. Structural comparison of A-platform binding sites for monovalent cations in the large ribosomal subunit (*A*) and the P4-P6 domain of the group I intron from *Tertrahymena thermophila* (*B*). Coordinates for (*B*) were taken from PDB #1GID. In both cases the AA-dinucleotide (red) is shown with surrounding RNA nucleotides (gray) and the monovalent cation (green).

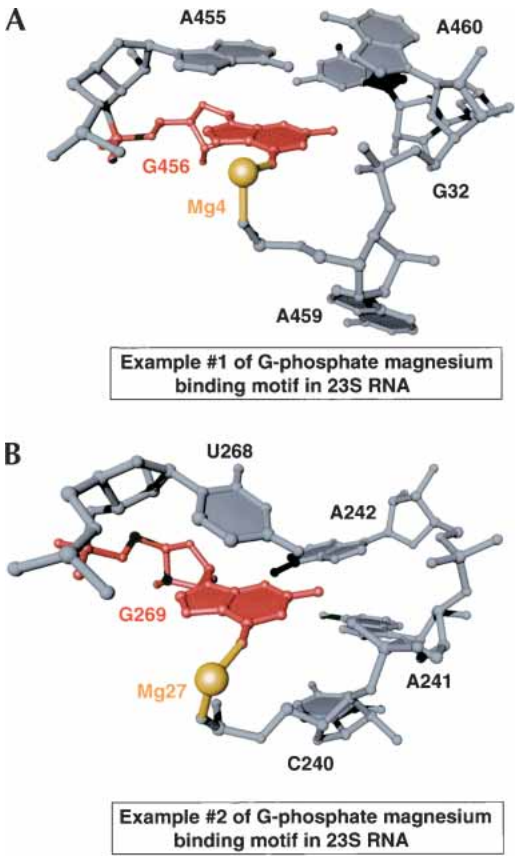

FIGURE 5. Structural comparison of two examples of a putative Mg^{2+} ion binding motif in 23S RNA. The G nucleotide (red) that coordinates the Mg^{2+} ion (gold) is shown in the context of surrounding nucleotides (gray).

somal subunit differ in the identity of the nucleotide that pairs with G, and in the sequential connectivity of the nucleotides that form their respective structure. Nonetheless, they are identical in their creation of a specific binding site that requires charge neutralization by a Mg^{2+} ion.

Metal ions that stabilize the tertiary and quaternary structures of the large ribosomal subunit

There are two general ways that metal ions stabilize the tertiary and quaternary structures of the large ribosomal subunit. First, metal ions indirectly affect tertiary interactions in 23S RNA by stabilizing local RNA secondary structures that are necessary for long-range intramolecular or intermolecular recognition. Second, metal ions appear in the interfaces between independently folded segments of RNA secondary structure as well as in the interfaces between ribosomal proteins and RNA, thereby directly stabilizing tertiary and quaternary structure.

Although it is impossible to know which metal ions in the large subunit are important for its structural stability, it seems likely that those bound to sites created by the packing of the domains of 23S RNA are critical. Eleven Mg^{2+} ions directly stabilize contacts between individual domains of 23S RNA through inner-sphere coordination, and 10 of them achieve this by coordination of nonbridging phosphate oxygen atoms. Nine of the 10 appear at the interfaces between domain II and one of the remaining domains of 23S RNA, and six of them are located between domains II and V, which is one of the largest and most conserved interfaces between domains. In particular, two partially dehydrated Mg^{2+} ions, one of type IIa (Mg13) and the other of type IIIa (Mg3), which are adjacent, form a core that nucleates the packing of the RNA backbones of helix 35.1 and helix 93 (Fig. 6A). Another nearby Mg^{2+} ion of type IIIb (Mg7) is bound to a conserved interface between domains II and IV, nucleating the packing of the RNA backbones of helix 35 and the terminal loop of helix 65 (Fig. 6A). Yet a fourth Mg^{2+} ion (Mg5) binds adjacent to the interface between domains II and IV to stabilize the secondary structure of the terminal loop of helix 65, which is presumably

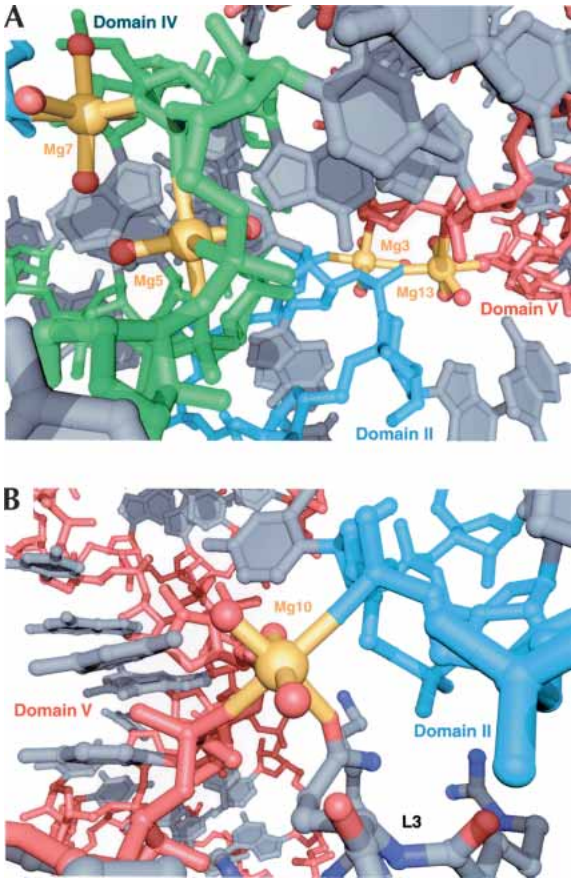

FIGURE 6. Magnesium ions that stabilize the tertiary and quaternary structures of the large ribosomal subunit. (*A*) A conserved interface between domains II (cyan), IV (green), and V (red) is shown with four Mg^{2+} ions (gold) that interact with the RNA backbone. All nucleotide bases are colored gray. (*B*) A Mg^{2+} ion (gold) that stabilizes an interface between domains II (cyan) and V (red), as well as ribosomal protein L3 (C atoms are gray, N atoms are blue, O atoms are red).

important for its tertiary interactions with domain V (Fig. 6A).

Six Mg^{2+} ions directly mediate contacts between 23S RNA and three ribosomal proteins through inner-sphere coordination. The interface between RNA and ribosomal protein L2 has three such Mg^{2+} ions, whereas the interfaces between RNA and L3 and L22 have two and one such Mg^{2+} ions, respectively. The most interesting and unique of these metal ion binding sites is one that contains a Mg^{2+} ion of type IIIa that bridges a conserved interface between domains II and V of 23S RNA and protein L3 (Fig. 6B). This Mg^{2+} ion makes inner-sphere contacts with nonbridging phosphate oxygen atoms in helix 35 and helix 90 and the side chain of Gln230 in L3. It appears that this Mg^{2+} ion is enabling the specific recognition of an RNA phosphate group by an amino acid side chain that would otherwise be incapable of such an interaction.

Outer-sphere contacts between Mg^{2+} ions and Na^+ ions also stabilize tertiary and quaternary contacts in the large ribosomal subunit. Ten Mg^{2+} ions mediate interactions between the domains of 23S RNA through outer-sphere contacts, and eight Na^+ ions do the same. In both cases we again find that the conserved interface between domains II and V is the most common location for such ions. Finally, 17 Mg^{2+} and 12 Na^+ ions mediate recognition of RNA by ribosomal proteins through outer-sphere coordination. In fact, 17 of the 29 proteins of the *H. marismortui* large subunit have at least one metal ion bound in their RNA interfaces.

Metal ions in the peptidyl transferase center

The concentration of metal ions in the structure of the large ribosomal subunit is highest in the regions of 23S RNA that are the most conserved across the three domains of life, mitochondria, and chloroplasts. Approximately half of the Mg^{2+} ions and one-third of the Na^+ ions found in the large ribosomal subunit interact with the peptidyl transferase center of domain V of 23S RNA and the conserved regions of domains II and IV that are immediately adjacent to the peptidyl transferase center. The high density of metal ions in this region is evident in Figure 7. The inner-sphere contacts in this part of 23S RNA are mapped out schematically in Figure 8, which documents the extraordinary degree to which Mg^{2+} ions and monovalent cations stabilize the interactions of many of the most conserved nucleotides in the ribosome. Approximately 40% of the nucleotides in the central loop of domain V make inner-sphere contacts with Mg^{2+}, Na^+, and K^+, and the fraction that are contacting metal ions increases when outer-sphere coordination is taken into account.

Helix 90 and its junction with the central loop of domain V has an especially large number of metal ions that stabilize its structure. This helix contains a number of bulged nucleotides that are stabilized by metal ions. One especially noteworthy nucleotide is G2618, whose phosphate group is surrounded by a cluster of three Mg^{2+} ions. Two of these Mg^{2+} ions are of type I, and each make a single inner-sphere contact to the pro(S) oxygen of G2618, whereas the third Mg^{2+} ion is of type IIa and coordinates the pro(R) oxygen of G2618 and the pro(R) oxygen of G2617. The many additional nucleotides that make outer-sphere contacts with these three Mg^{2+} ions suggest that they provide a critical charge neutralization function in this region of the peptidyl transferase center.

There is one noteworthy electron density peak in the peptidyl transferase center that would not have an obvious structural role if it were modeled as a metal ion. This electron density peak appears at 1.6σ in experimentally phased maps, but becomes much stronger (3.9σ) in refined $2F_{obs}$-F_{calc} maps. It is spherical, and does not have features typical of a Mg^{2+} ion. Further, this peak does not correspond to a site of isomorphous difference with crystals containing Rb^+. Therefore, if this peak is a K^+ ion, then this K^+ ion does not appear to be substituted with Rb^+. A water molecule (HOH 75) has been modeled into this electron density peak, but the temperature factor for this water molecule after crystallographic refinement is 14 $Å^2$, which is much lower than temperature factors observed for RNA in this region (~30 $Å^2$). This peak is 3.1 Å from the 2′-hydroxyl of C2104, which is the only ligating group in RNA for this peak. The temperature factor of the 2′-hydroxyl group of C2104 is ~34 $Å^2$. These data suggest that this electron density peak is not a water molecule, and is instead an ion more electron-dense than oxygen, the identity of which we do not currently know. It is possible that it may be a chloride ion, as similar coordination ligands in RNA have recently been observed to bind chloride (Auffinger et al. 2004). Nevertheless, given that this ion is 4.4 Å from the 3-imino group of A2486, which has been implicated in the catalysis of nascent peptide bond formation, future experiments must be done to clarify its identity. However, a catalytic role for this ion already seems unlikely, as the structure of the CCA-phe-cap-biotin substrate analog bound to the large subunit's P-site (Schmeing et al. 2002) places the 3-imino group of A76 only 1.6 Å from the position of this ion, suggesting that this ion cannot occupy the same position in ribosomes containing bound substrates.

DISCUSSION

The importance of metal ions for ribosome structure and function

The identification of structural metal ions in the *H. marismortui* large ribosomal subunit can account for the biochemical observations that the ribosome is remarkably sensitive to ionic conditions. The basic functional groups of the ribosomal proteins are insufficient to neutralize all of the closely juxtaposed electronegative functional groups produced by the folding and packing of 23S RNA. For this

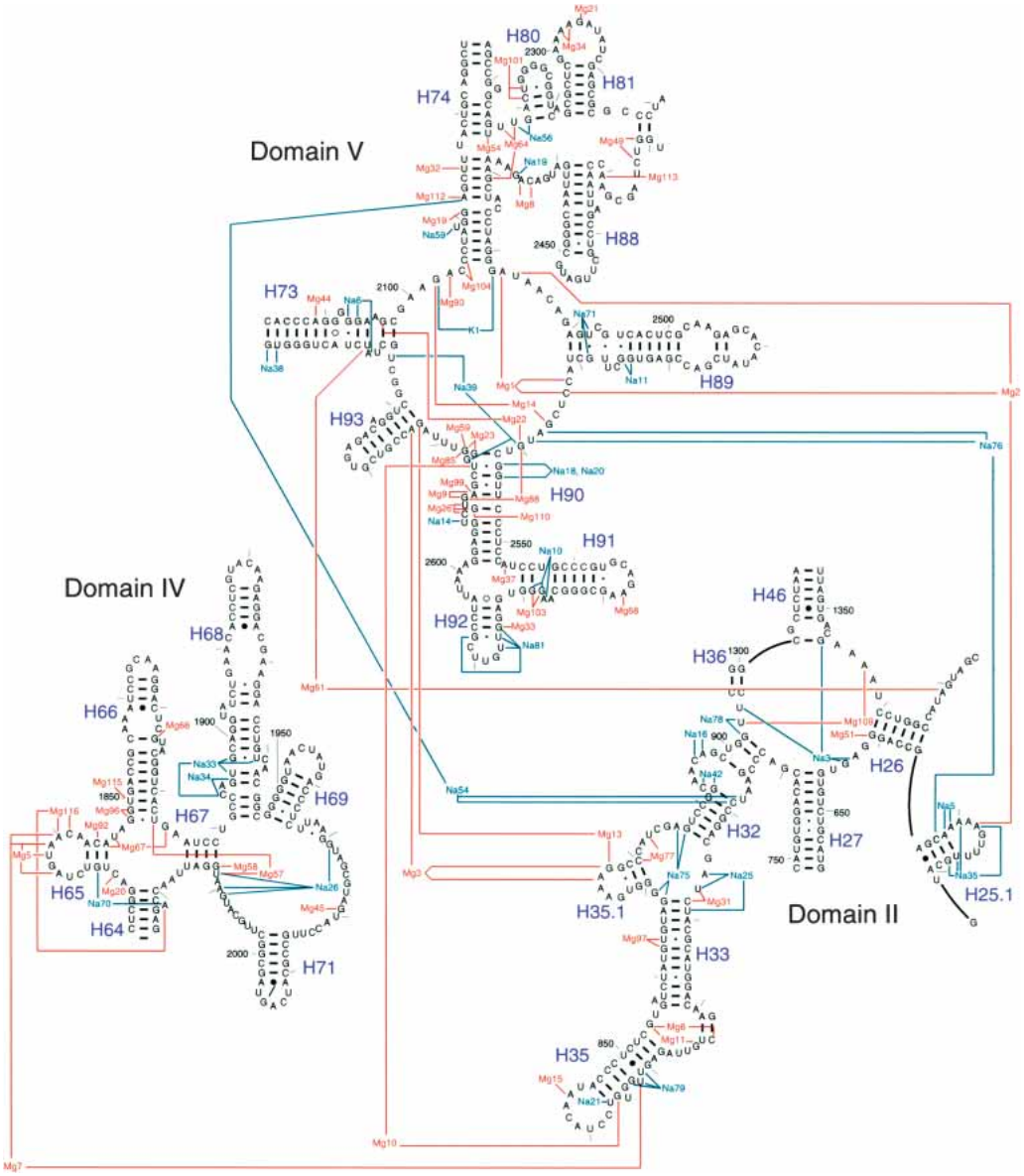

FIGURE 7. Secondary structure diagram showing the metal ion binding sites present in the most conserved regions of 23S RNA. Nucleotides shown are 619–656, 749–906, 1299–1308, 1346–1374 in domain II, 1824–2025 in domain IV, and 2084–2127, 2266–2321, and 2419–2660 in domain V (*H. marismortui* numbering). Only nucleotides that coordinate the inner sphere of Mg^{2+} ions are shown connected to the ion.

reason, metal ions are essential for the structural integrity of the ribosome, and consequently, its functional activity. A loss of metal ions from many of the observed binding sites would most likely lead to significant denaturation of the large subunit, including the unfolding of the domains of 23S RNA, loss of ribosomal proteins, and destabilization of RNA secondary structure. Therefore, the loss of ribosomal function known to occur in the absence of various metal ions, including the loss of peptidyl transferase activity, appears best explained by indirect structural perturbations.

Essentially all of the distinct functional regions of the peptidyl transferase center appear to depend heavily on metal ions for their structural stability. This is most likely the result of the notable absence of ribosomal proteins in this region, and illustrates the degree to which complex tertiary folds in RNA are dependent on metal ions. Therefore, although compelling evidence exists that a primordial ribosome lacked ribosomal proteins, these results unequivocally demonstrate that an all-RNA ribosome would have depended on metal ions for its structural integrity.

The structure of the large ribosomal subunit further demonstrates that specificity for certain metal ions is achieved by numerous metal ion binding sites in the ribosome. The solution used to stabilize our crystals contained 1.7 M NaCl, 0.5 M NH_4Cl, 0.1 M KCl, and 0.03 M $MgCl_2$ and would therefore favor the binding of monovalent cat-

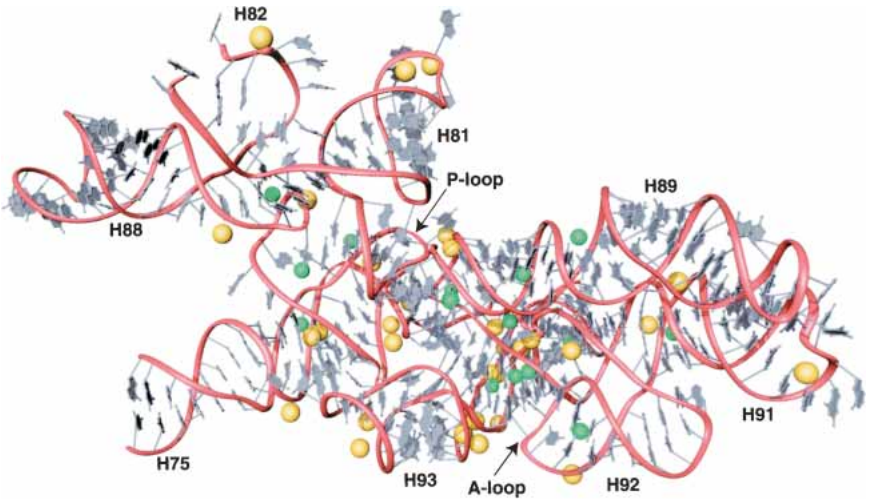

FIGURE 8. Three-dimensional representation showing the metal ion binding sites present in the peptidyl transferase center. The RNA backbone (red) is shown with bases (gray), Mg^{2+} ions (gold), and monovalent cations (green). Nucleotides shown are 2084–2127, 2266–2321, and 2419–2660 (*H. marismortui* numbering).

ions to binding sites that are nonspecific with respect to monovalent or divalent metal ions. The unambiguous identification of Mg^{2+} ions to 116 distinct binding sites indicates that Na^+, NH_4^+, and K^+ cannot substitute for Mg^{2+} at such sites. Therefore, among these sites are those whose loss leads to perturbation of the structure when Mg^{2+} is depleted from solutions used for ribosome preparation.

The specificity of 86 binding sites for Na^+ is more difficult to evaluate, because of the ionic conditions used to prepare our crystals. Na^+ is likely to dominate in sites that might prefer to interact with Mg^{2+} under more normal ionic conditions. The Na^+ ion binding sites at the major groove edge of guanosines in G-U wobble base pairs provide a case in point. In previous work, the major groove edge of tandem G-U wobble pairs was found to be a binding site for cobalt hexamine and hexahydrated magnesium (Cate and Doudna 1996; Kieft and Tinoco 1997). However, in the *H. marismortui* large ribosomal subunit such sites are rarely occupied by $Mg^{2+}(H_2O)_6$. Interestingly, it has been reported that such sites can be occupied by either Mg^{2+} or K^+ in the structure of a fragment of the signal recognition particle RNA (Batey and Doudna 2002). Therefore, the most likely explanation for the Na^+ ion preference we observe in these sites is their lack of absolute specificity, not the absence of a preference for Mg^{2+}. In other Na^+ binding sites in the large subunit, coordination distances and geometries suggest a true selectivity for monovalent cations (e.g., Figs. 3B, 4B).

Does the large ribosomal subunit contain binding sites for metal ions in addition to those already identified? It has been reported that 20% of RNA phosphates in the ribosome are neutralized specifically by Mg^{2+} (Weiss et al. 1973), although others report values ranging from 8% to 17% (Hurwitz and Rosano 1967; Lusk et al. 1968). The 116 Mg^{2+} ions identified in the crystal structure are only enough to compensate for ~8% of the nucleotides in 23S RNA if a ratio of one Mg^{2+} ion per two nucleotides is assumed. In fact, the phosphate groups of 263 different nucleotides in 23S RNA (~9%) interact with Mg^{2+} ions. However they are counted, the number of Mg^{2+} ions observed localized in a specific position is lower than expected from previous biochemical measurements. This smaller number may reflect the difficulty of unambiguously identifying metal ions in regions where the quality of electron density maps is low, or it could result from some Mg^{2+} ions occupying less specifically localized positions. The former is the likely explanation for why previously reported metal ions in the L11 binding region of 23S rRNA (Conn et al. 2002) are not clearly visible in the current electron density maps for the large subunit.

The periphery of the large ribosomal subunit is a region where undetected Mg^{2+} ion binding sites are most likely to exist. For example, we did not find any Mg^{2+} ions on the surface of the large ribosomal subunit that contacts the small subunit, the region where the Mg^{2+} ions required for subunit interactions are likely to bind. This surface of the 50S subunit is accessible to solvent channels in the crystal, and consequently one would expect Mg^{2+} ions in this region to interact in a "diffuse binding" mode, which would not yield distinct electron density peaks. It is also possible that these sites may exist only in the intact 70S ribosome.

Principles of metal ion binding to large RNAs

The crystal structure of the P4-P6 domain of the group I intron, which contains 158 nucleotides, provided significant insights into the ways in which metal ions stabilize the tertiary structure of large RNAs (Cate et al. 1996). An examination of metal binding sites in the P4-P6 domain revealed that Mg^{2+} ions principally bind in the major groove of RNA helices (Cate and Doudna 1996), although an additional Mg^{2+} ion core was observed and proposed to serve as an RNA counterpart to the hydrophobic core found in proteins (Cate et al. 1997). These results were supported by a more recent 2.25 Å crystal structure of the P4-P6 domain that revealed 27 Mg^{2+} ions and numerous water molecules located on the interior of the RNA structure, suggesting an important role for these in the proper folding of large RNA molecules (Juneau et al. 2001). The identification of metal ions in the large ribosomal subunit which includes 2876 nucleotides of RNA has provided a wealth of new informa-

tion about the roles of metal ions in stabilizing the structure of large RNAs.

As in the P4-P6 domain, the large ribosomal subunit structure suggests that metal ion cores contribute to the nucleation and tertiary packing of RNA helices. Using our proposed structural classification, the types of Mg^{2+} ion binding sites usually found in such metal ion cores of 23S RNA are frequently of types III and IV. Moreover, we observe metal ion binding sites created by nucleotides that are separated by vast stretches of RNA sequence, in some cases > 1000 nucleotides. The tertiary fold of 23S RNA in numerous regions, but most significantly in the peptidyl transferase center, is impossible without a multitude of precisely positioned structural metal ions that include Na^+, K^+, and Mg^{2+}. Therefore, in addition to long-range Watson-Crick base-pairs and A-minor interactions (Nissen et al. 2001), the tertiary structure of large RNAs is undoubtedly mediated and stabilized by site-bound metal ions.

Metal ions appear critical for the quaternary structure of the ribosome, as they are found at numerous interfaces between 23S RNA and ribosomal proteins. In previously determined structures of proteins complexed with RNA, metal ions are typically required to stabilize the structure of the RNA needed for specific protein recognition. Whereas numerous metal ions perform similar functions in the large subunit, a large number of metal ions directly stabilize intermolecular contacts between ribosomal proteins and RNA.

MATERIALS AND METHODS

Crystals of the *H. marismortui* large ribosomal subunit were grown and stabilized as described (Ban et al. 2000). Crystals containing bound Rb^+ ions were prepared by gradual transfer into a solution containing 1 M RbCl, 100 mM NH_4-acetate, 30 mM $MgCl_2$, 20 mM MES-Tris, pH 6.2, 12% PEG 6000, and 20% ethylene glycol before flash-freezing in liquid propane. Diffraction data for crystals soaked in RbCl were collected using beamline X12B at the National Synchrotron Light Source of Brookhaven National Laboratory, Brookhaven, NY, with a 1.38 Å wavelength. Data reduction was done with DENZO and scaled with SCALEPACK (Otwinowski and Minor 1987) using a resolution range of 30–3.5 Å. Data completeness was 97.6% with an average I/σ of 5.2 and R_{sym} of 15.6%. For the resolution shell between 3.56 Å and 3.50 Å, completeness was 91.1% with an average I/σ of 1.6 and R_{sym} of 50.8%. Isomorphous difference electron density maps were calculated with CNS (Brunger et al. 1998) using experimental phases. Interpretation of electron density and modeling of ions was done using the program O (Jones et al. 1991). The complete atomic coordinates of the large subunit containing all metal ions have been deposited in the Protein Data Bank (PDB ID code 1s72).

ACKNOWLEDGMENTS

We thank Poul Nissen for collecting the data for RbCl soaked crystals, and for many helpful discussions, as well as Martin Schmeing for many helpful discussions. This work was supported by a National Institutes of Health (NIH) grant (GM22778) and a grant from the Agouron Institute. D.J.K. is a Howard Hughes Medical Institute (HHMI) predoctoral fellow.

The publication costs of this article were defrayed in part by payment of page charges. This article must therefore be hereby marked "advertisement" in accordance with 18 USC section 1734 solely to indicate this fact.

Received March 25, 2004; accepted June 21, 2004.

REFERENCES

Auffinger, P., Bielecki, L., and Westhof, E. 2004. Anion binding to nucleic acids. *Structure* **12:** 379–388.

Ban, N., Nissen, P., Hansen, J., Moore, P.B., and Steitz, T.A. 2000. The complete atomic structure of the large ribosomal subunit at 2.4 Å resolution. *Science* **289:** 905–920.

Basu, S., Rambo, R.P., Strauss-Soukup, J., Cate, J.H., Ferre-D'Amare, A.R., Strobel, S.A., and Doudna, J.A. 1998. A specific monovalent metal ion integral to the AA platform of the RNA tetraloop receptor. *Nat. Struct. Biol.* **5:** 986–992.

Batey, R.T. and Doudna, J.A. 2002. Structural and energetic analysis of metal ions essential to SRP signal recognition domain assembly. *Biochemistry* **41:** 11703–11710.

Brunger, A.T., Adams, P.D., Clore, G.M., DeLano, W.L., Gros, P., Grosse-Kunstleve, R.W., Jiang, J.S., Kuszewski, J., Nilges, M., Pannu, N.S., et al. 1998. Crystallography & NMR system: A new software suite for macromolecular structure determination. *Acta Crystallogr. D Biol. Crystallogr.* **54:** 905–921.

Cate, J.H. and Doudna, J.A. 1996. Metal-binding sites in the major groove of a large ribozyme domain. *Structure* **4:** 1221–1229.

Cate, J.H., Gooding, A.R., Podell, E., Zhou, K., Golden, B.L., Kundrot, C.E., Cech, T.R., and Doudna, J.A. 1996. Crystal structure of a group I ribozyme domain: Principles of RNA packing. *Science* **273:** 1678–1685.

Cate, J.H., Hanna, R.L., and Doudna, J.A. 1997. A magnesium ion core at the heart of a ribozyme domain. *Nat. Struct. Biol.* **4:** 553–558.

Chao, F.C. 1957. Dissociation of macromolecular ribonucleoprotein of yeast. *Arch. Biochem. Biophys.* **70:** 426–431.

Chao, F.C. and Schachman, H.K. 1956. The isolation and characterization of a macro-molecular ribonucleoprotein from yeast. *Arch. Biochem. Biophys.* **61:** 220–230.

Conn, G.L., Gittis, A.G., Lattman, E.E., Misra, V.K., and Draper, D.E. 2002. A compact RNA tertiary structure contains a buried backbone-K^+ complex. *J. Mol. Biol.* **318:** 963–973.

Gordon, J. and Lipmann, F. 1967. Role of divalent ions in poly U-directed phenylalanine polymerization. *J. Mol. Biol.* **23:** 23–33.

Hurwitz, C. and Rosano, C.L. 1967. The intracellular concentration of bound and unbound magnesium ions in *Escherichia coli*. *J. Biol. Chem.* **242:** 3719–3722.

Jones, T.A., Zou, J.Y., Cowan, S., and Kjeldgaard, M. 1991. Improved methods for building proteins models in electron density maps and the location of errors in these models. *Acta Crystallogr.* **A46:** 110–119.

Juneau, K., Podell, E., Harrington, D.J., and Cech, T.R. 2001. Structural basis of the enhanced stability of a mutant ribozyme domain and a detailed view of RNA-solvent interactions. *Structure* **9:** 221–231.

Khawaja, J.A. and Raina, A. 1970. Effect of spermine and magnesium on the attachment of free ribosomes to endoplasmic reticulum membranes. *Biochem. Biophys. Res. Commun.* **41:** 512–518.

Kieft, J.S. and Tinoco Jr., I. 1997. Solution structure of a metal-binding site in the major groove of RNA complexed with cobalt (III) hexammine. *Structure* **5:** 713–721.

Kimes, B.W. and Morris, D.R. 1973. Cations and ribosome structure. II. Effects on the 50S subunit of substituting polyamines for mag-

nesium ion. *Biochemistry* **12:** 442–449.
Lusk, J.E., Williams, R.J., and Kennedy, E.P. 1968. Magnesium and the growth of *Escherichia coli. J. Biol. Chem.* **243:** 2618–2624.
McCarthy, B.J. 1962. Effects of magnesium starvation on ribosome content of *Escherichia coli. Biochim. Biophys. Acta.* **55:** 880–888.
Misra, V.K. and Draper, D.E. 1999. On the role of magnesium ions in RNA stability. *Biopolymers* **48:** 113–135.
Moore, P.B. 1966. Polynucleotide attachment to ribosomes. *J. Mol. Biol.* **18:** 8–20.
Naslund, P.H. and Hultin, T. 1970. Effects of potassium deficiency on mammalian ribosomes. *Biochim. Biophys. Acta.* **204:** 237–247.
———. 1971. Structural and functional defects in mammalian ribosomes after potassium deficiency. *Biochim. Biophys. Acta.* **254:** 104–116.
Nissen, P., Hansen, J., Ban, N., Moore, P.B., and Steitz, T.A. 2000. The structural basis of ribosome activity in peptide bond synthesis. *Science* **289:** 920–930.
Nissen, P., Ippolito, J.A., Ban, N., Moore, P.B., and Steitz, T.A. 2001. RNA tertiary interactions in the large ribosomal subunit: The A-minor motif. *Proc. Natl. Acad. Sci.* **98:** 4899–4903.
Otwinowski, Z. and Minor, W. 1987. Processing of X-ray diffraction data collected in oscillation mode. *Methods Enzymol.* **276:** 307–326.
Pyle, A.M. 2002. Metal ions in the structure and function of RNA. *J. Biol. Inorg. Chem.* **7:** 679–690.
Schmeing, T.M., Seila, A.C., Hansen, J.L., Freeborn, B., Soukup, J.K., Scaringe, S.A., Strobel, S.A., Moore, P.B., and Steitz, T.A. 2002. A pre-translocational intermediate in protein synthesis observed in crystals of enzymatically active 50S subunits. *Nat. Struct. Biol.* **9:** 225–230.
Shiman, R. and Draper, D.E. 2000. Stabilization of RNA tertiary structure by monovalent cations. *J. Mol. Biol.* **302:** 79–91.
Tissieres, A., Watson, J.D., Schlessinger, D., and Hollingworth, B.R. 1959. Ribonucleoprotein particles from *Escherichia coli. J. Mol. Biol.* **1:** 221–233.
Wacker, W.E. 1969. The biochemistry of magnesium. *Ann. N. Y. Acad. Sci.* **162:** 717–726.
Weiss, R.L., Kimes, B.W., and Morris, D.R. 1973. Cations and ribosome structure. 3. Effects on the 30S and 50S subunits of replacing bound Mg^{2+} by inorganic cations. *Biochemistry* **12:** 450–456.
Zitomer, R.S. and Flaks, J.G. 1972. Magnesium dependence and equilibrium of *Escherichia coli* ribosomal subunit association. *J. Mol. Biol.* **71:** 263–279.